ASYMPTOTIC ANALYSIS AND REDUCED-ORDER MODELING OF A PASSIVE THROTTLE-BASED TEMPERATURE FLOW COMPENSATOR

Rumen Yankov[1], Ventsislav Dimitrov[2] [https://orcid.org/0009-0006-9667-8028], Veselina Dimitrova[3] [https://orcid.org/0009-0001-0157-1775], Konstantin Raykov[4], Georgi Tonkov[5], Sylvester Bozherikov[6] [https://orcid.org/0009-0003-0004-9912], Gergana Tonkova[7]
[1]College Sliven, Technical University of Sofia, Sliven, Bulgaria, EU
[2,3,4,6]Department MEMETE, Faculty of Engineering and Pedagogy of Sliven, TU of Sofia, Bulgaria
[5]Faculty of Mechanical Engineering, Technical University of Sofia, Sofia, Bulgaria, EU
[7]Faculty of Mining Electromechanics, University of Mining and Geology "St. Ivan Rilski", Sofia, Bulgaria, EU
Emails: r.yankov@tu-sofia.bg, vpdd_acad@tu-sofia.bg, vkdd_acad@tu-sofia.bg, k.raykov@tu-sofia.bg, gptonkov@tu-sofia.bg, s.bozherikov@tu-sofia.bg, gtonkova@mgu.bg

Abstract - Temperature-induced variations in fluid properties represent a major source of flow-rate instability in throttle-based hydraulic systems operating under constant pressure drop conditions. This study develops a comprehensive analytical framework for a passive throttle-based temperature flow compensator by combining quasi-static modeling, asymptotic analysis, and reduced-order fluid–structure interaction (FSI) dynamics. The operating principle of the compensator is described using a quasi-static equilibrium formulation based on nonlinear laminar and turbulent throttling laws and mechanical force balance. Temperature-dependent effects are incorporated through asymptotic expansions of fluid properties and pressure redistribution parameters, yielding explicit analytical expressions for plunger displacement, throttling flow rate, and temperature sensitivity. The asymptotic formulation enables analytical assessment of monotonicity, uniqueness of equilibrium solutions, and robustness of the compensator response with respect to thermal variations. To extend the analysis beyond equilibrium conditions, a reduced-order FSI model is formulated as a coupled system of ordinary differential equations describing chamber pressure dynamics and plunger motion, including inertia and damping effects. The quasi-static equilibrium is recovered as the steady-state solution of the dynamic model, ensuring consistency between static and dynamic descriptions. Validation of the proposed framework is achieved through comparison between the quasi-static model, the asymptotic approximation, and the reduced-order FSI model, supported by representative numerical evaluations of equilibrium displacement and transient response characteristics. The results demonstrate that the proposed approach provides a physically interpretable and computationally efficient tool for the analysis and design of passive temperature flow compensators, offering clear insight into equilibrium sensitivity, dynamic stability, and practical applicability in hydraulic systems.

Keywords: Asymptotic analysis; Reduced-order modeling; Passive flow compensator; Nonlinear hydraulics; Temperature effects; Equilibrium stability.

1. Introduction

Temperature variations of the working fluid are a key factor affecting the performance and reliability of hydraulic systems. Changes in viscosity and density influence flow resistance, leakage, and pressure distribution within hydraulic chambers, causing deviations in delivered flow even under constant operating conditions. Early studies demonstrated that, even at constant pressure drop, fluid temperature significantly affects chamber pressure and flow, revealing the physical origin of temperature-induced flow instability [1].

Classical hydraulic theory attributes these effects mainly to the temperature dependence of viscosity, which governs laminar-to-turbulent transitions and corresponding resistance laws. Foundational works in technical hydromechanics and hydraulic

dx.doi.org/10.17683/ijomam/issue23.5

machinery describe linear (laminar) and quadratic (turbulent) throttling, as well as equilibrium conditions from pressure and force balances in hydraulic elements [2–4]. These relations underpin the design of throttle-based flow control devices with prescribed pressure–flow characteristics [5].

Two strategies mitigate temperature-induced performance degradation. Active control involves fluid temperature regulation or electronically controlled valves with adaptive flow correction. Passive hydraulic–mechanical solutions rely on internal force balance between pressure-generated forces and a restoring element, typically a spring [1,3,6]. Passive compensators are attractive for their simplicity, robustness, and independence from sensors or electronic control [7].

Early analytical models of passive compensators are quasi-static, using algebraic relations between pressures, flow, and mechanical displacement. Characteristics were often obtained graphically or semi-analytically, limiting assessment of parameter sensitivity, uniqueness, and stability [2,3,5]. Nevertheless, these models laid the groundwork for systematic design and remain influential in practice.

Recent trends favor reduced-order (lumped-parameter) models, describing coupled dynamics of pressure, flow, and mechanical motion using compact ordinary differential equations. These allow transparent interpretation, analysis of transient behavior, stability, and parameter robustness [8–11], serving as practical alternatives to full-scale simulations.

Asymptotic and perturbation methods are increasingly applied to nonlinear fluid–mechanical systems. These frameworks exploit small parameters and scale separation to derive approximate closed-form solutions, systematically incorporating temperature-dependent fluid properties and flow coefficients [12–14]. Asymptotic analysis enables conditions for monotonicity and uniqueness of equilibrium solutions, identification of regimes avoiding multiple equilibria [15,16], and supports local stability analysis and detection of bifurcations [17,18].

Experimental and numerical studies confirm that temperature variations significantly affect volumetric losses and flow characteristics, emphasizing the need for effective compensation mechanisms [19–21]. Passive throttle-based compensators are particularly promising, offering flow correction without additional complexity or active control loops [7,22].

Contemporary research highlights reduced-order and lumped-parameter modeling as efficient tools for analytical investigation, optimization, and stability assessment of fluid power systems [23–25], capturing essential nonlinear interactions between flow dynamics and mechanical motion.

Alongside physics-based modeling, data-driven and neural-network-based approaches have been applied to system characterization and parameter identification [26], while analytical studies of Cohen–Grossberg-type bidirectional associative memory neural networks emphasize stability-oriented reduced-order modeling but lack the physical interpretability and explicit sensitivity information required for analytical assessment of hydraulic compensation mechanisms [27].

Recent experimental and analytical studies have demonstrated that temperature effects and dynamic interactions critically influence the performance and stability of hydraulic systems. Significant temperature-dependent changes in volumetric efficiency and flow characteristics of variable-speed pumps have been reported in the literature, while pronounced thermal effects on gear pump performance have also been observed [28]. Furthermore, temperature-induced deviations in the flow mapping of electrohydraulic control elements have been shown to require explicit consideration in control-oriented modeling [29], and it has been confirmed that temperature-dependent hydraulic and mechanical parameters strongly affect transient response and stability margins [30].

Despite extensive literature, a comprehensive analytical treatment of passive throttle-based temperature flow compensators is still lacking, particularly frameworks combining nonlinear throttling laws, mechanical force balance, and temperature-dependent fluid properties to yield explicit expressions for equilibrium, sensitivity, and stability [31–33]. The present study addresses this gap by developing an asymptotic and reduced-order modeling framework. Starting from a quasi-static equilibrium formulation, temperature-dependent fluid properties are incorporated via asymptotic expansions to obtain closed-form expressions for plunger displacement and flow rate. A reduced-order fluid–structure interaction model is also introduced to analyze transient behavior and stability, providing a rigorous basis for passive temperature compensation in hydraulic systems.

2. Fundamental Quasi-Static Model of the Throttle-Based Temperature Flow Compensator

Variations in the temperature of the working fluid have a pronounced influence on the volumetric losses in hydraulic machines and control devices, which leads to deterioration of the performance characteristics of hydraulic drive systems. Compensation of this effect may be achieved either by stabilizing the temperature of the working fluid or by incorporating hydraulic devices capable of compensating temperature-induced variations in volumetric losses.

In [1], the influence of working-fluid temperature on the pressure in a flow-through hydraulic chamber

was investigated experimentally. On the basis of these results, a throttle-based temperature flow compensator was proposed. A characteristic feature of the compensator is the presence of two throttling elements with different hydraulic behavior: one laminar (linear) and one turbulent (quadratic).

The experimental investigation was carried out over a temperature interval of 26–78 °C, under a constant pressure drop p_1-p_2=0.2 MPa, using standard light-grade mineral hydraulic oil. Within this interval, the pressure in the flow-through chamber exhibits an approximately linear dependence on temperature, characterized by a nearly constant gradient:

$$\left|\frac{d_{pk}}{dt}\right| = 8{,}3kPa/°C \tag{1}$$

Figure 1 shows the scheme of the hydraulic throttle temperature compensator developed by the author, whose task is to increase the flow rate to the hydraulic system by a value corresponding to the increase in volumetric losses resulting from the increase in the temperature of the working fluid.

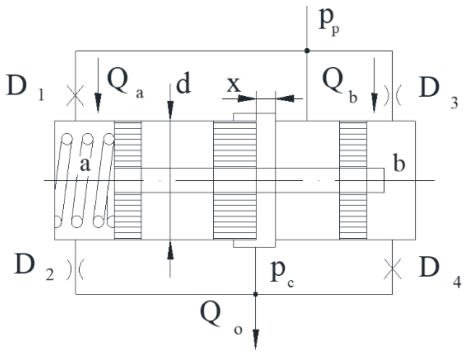

Figure 1: Schematic diagram and operating principle of the throttle-based temperature flow compensator

Flow chambers (a) and (b) are formed on both sides of the plunger. According to the scheme, a turbulent (quadratic) throttle D_1 is installed at the inlet of chamber (a), and a laminar (linear) throttle D_2 is installed at the outlet. A compression spring is installed in chamber (a).

In the idle position, the spring holds the plunger against the right stop, which corresponds to zero displacement x=0 and a minimum value of the flow rate of the flowing fluid. With this connection scheme, as the temperature increases, the pressure pap_apa in chamber (a) decreases, while that in chamber (b), pbp_bpb, increases. Thus, a displacement of the plunger to the left can be caused, respectively increasing the fluid flow rate.

At a reference temperature $t=t_0$, the pressures in the two chambers are assumed equal:

$$p_a = p_b = \frac{p_p+p_c}{2}\Big|_{t=t_0} \tag{2}$$

where:

-p_p,p_c – inlet and outlet pressures [Pa],

- p_a,p_b – chamber pressures [Pa].

For an increase in temperature of Δt, the resultant force generated by the pressure difference acting on the plunger faces is assumed to be equal to the spring force corresponding to the initial compression x_0:

$$(p_b-p_a)\frac{\pi D^2}{4} = cx_0|_{t=t_0+\Delta_t} \tag{3}$$

For temperatures exceeding t_0+Δt, the plunger occupies an equilibrium position corresponding to an additional compression x of the spring. Neglecting friction, the force balance yields

$$(p_b-p_a)\frac{\pi D^2}{4} = c(x_0+x) \tag{4}$$

where:

- D,d – plunger and throttling diameters [m],

- x,x_0 – additional and initial spring compression [m].

- c – spring constant [N/m].

Using the expressions for pap_apa and pbp_bpb derived in [1] and substituting them into Eq. (4), the plunger displacement is obtained in the form:

$$x = \frac{\left[p_p-p_c+A^2-A\sqrt{4(p_p-p_c)+A^2}\right]\pi d^2}{4c} - x_0 \tag{5}$$

which represents a functional dependence of the form x=x[A(t)].

The total flow rate through the compensator is expressed as:

$$Q_0 = Q_a+Q_b+Q_{throt} \tag{6}$$

where the throttling contribution is given by:

$$Q_{throt} = \eta\pi d_x\sqrt{\frac{2}{\rho}(p_p-p_c)} = \eta f_{throt}\sqrt{\frac{2}{\rho}(p_p-p_c)} \tag{7}$$

where:

- $f_{throt}=\pi d_x f$ denoting the throttling area.

- A(t)– temperature-dependent parameter from [1]

- η – discharge coefficient [-]

- ρ(t) – fluid density [kg/m^3]

The total flow rate may further be decomposed as:

$$Q_0 = \Delta Q_{lost}(t)+Q_{work} \tag{8}$$

where:

- Q_a,Q_b,Q_{throt},Q_0,Q_{work} – flow rates [m^3/s]

- ΔQ_{lost} – temperature-dependent volumetric losses [m^3/s].

The volumetric losses $\Delta Q_{lost}(t)$ depend explicitly on temperature, while the working flow rate Q_{work} is

determined by the operating requirements of the driven hydraulic motor. From Eqs. (6)–(8), the throttling area as a function of temperature follows as:

$$f_{throt} = \frac{\Delta Q_{lost}(t) + Q_{work} - 2Q_a(t)}{\eta\sqrt{\frac{2}{\rho}(p_p - p_c)}} \quad (9)$$

The relations (5)–(9) define a closed quasi-static model of the throttle-based temperature flow compensator. For unambiguous correction of the flow rate as a function of temperature alone, the pressure difference must satisfy the condition:

$$p_p - p_c = const \quad (10)$$

3. Asymptotic Analysis of the Quasi-Static Equilibrium

The quasi-static formulation developed in Section 2 provides a verified baseline description of the equilibrium behavior of the throttle-based temperature flow compensator. However, the equilibrium displacement and flow rate are obtained implicitly and are typically evaluated by graphical–analytical procedures, which limits their suitability for systematic sensitivity analysis and analytical generalization. To overcome these limitations, an asymptotic approach is introduced in the present section, enabling explicit analytical representation of the equilibrium response under weak temperature variations.

According to Section 2, the temperature dependence of the equilibrium enters the compensator response through the temperature-dependent parameter A(t), the chamber flow term Qa(t), the volumetric losses $\Delta Q_{lost}(t)$, and the fluid density ρ(t). All symbols, assumptions, and governing relations of Section 2 are retained without modification. In particular, the pressure drop $\Delta p = p_p - p_c$ is assumed constant.

A small thermal perturbation about a reference operating temperature $t = t_0$ is introduced as:

$$t = t_0 + \varepsilon\theta \quad (11)$$

where $\varepsilon \ll 1$ is a dimensionless bookkeeping parameter quantifying weak temperature variations and $\theta = \mathcal{O}(1)$ is a scaled temperature variable.

The temperature-dependent parameter A(t), introduced in Section 2 through the pressure redistribution model of [1], is expanded as a regular series:

$$A(t) = A_0 + \varepsilon A_1(\theta) + \varepsilon^2 A_2(\theta) + \cdots, \quad (12)$$

where $A_0 = A(t_0)$. The fluid density ρ(t), expressed in kg/m³, is expanded as:

$$\rho(t) = \rho_0 + \varepsilon\rho_1(\theta) + \varepsilon^2\rho_2(\theta) + \cdots, \quad (13)$$

with $\rho_0 = \rho(t_0)$. The chamber flow term Qa(t) and the volumetric losses $\Delta Q_{lost}(t)$, both defined in Section 2, are expanded as:

$$Q_a(t) = Q_{a_0} + \varepsilon Q_{a1}(\theta) + \varepsilon^2 Q_{a2}(\theta) + \cdots, \quad (14)$$

$$\Delta Q_{lost}(t) = \Delta Q_{lost_0} + \varepsilon\Delta Q_{lost_1}(\theta) + \cdots, \quad (15)$$

From Eq. (5) of Section 2, introduce the nonlinear mapping:

$$\Phi(A) = \frac{\left[p_p - p_c + A^2 - A\sqrt{4(p_p - p_c) + A^2}\right]\pi d^2}{4c} \quad (16)$$

where d is the throttling diameter and c is the spring stiffness. The plunger displacement x(t), measured in meters, is given by:

$$x(t) = \Phi\big(A(t)\big) - x_0, \quad (17)$$

with x_0 denoting the initial spring pre-compression.

Here, Φ(A) represents the nonlinear displacement mapping induced by the pressure redistribution parameter A(t), while x(t) denotes the plunger displacement measured from the reference stop.

Expanding Φ(A(t)) about A_0 yields:

$$x(t) = x^{(0)} + \varepsilon x^{(1)}(\theta) + \varepsilon^2 x^{(2)}(\theta) + \cdots, \quad (18)$$

where:

$$x^{(0)} = \Phi(A_0) - x_0, \quad (19)$$

$$x^{(1)} = \Phi'(A_0)A_1(\theta), \quad (20)$$

$$x^{(2)} = \Phi'(A_0)A_2(\theta) + \frac{1}{2}\Phi''(A_0)[A_1(\theta)]^2 \quad (21)$$

The throttling contribution to the total flow rate, defined in Section 2, reads

$$Q_{throt}(t) = \eta\pi d_x(t)\sqrt{\frac{2}{\rho(t)}(p_p - p_c)} \quad (22)$$

where η is the discharge coefficient. Introducing the reference factor:

$$S_0(t) = \sqrt{\frac{2}{\rho(t)}(p_p - p_c)} \quad (23)$$

and expanding $\rho(t)^{-1/2}$, one obtains:

$$Q_{throt}(t) = Q_{throt}{}^{(0)} + \varepsilon Q_{throt}{}^{(1)}(\theta) + \varepsilon^2 Q_{throt}{}^{(2)}(\theta) + \cdots, \quad (24)$$

with:

$$Q_{throt}{}^{(0)} = \eta\pi d x^{(0)} S_0 \quad (25)$$

$$Q_{throt}{}^{(1)}(\theta) = \eta\pi d S_0\left[x^{(1)}(\theta) - \frac{1}{2}x^{(0)}\frac{\rho_1(\theta)}{\rho_0}\right] \quad (26)$$

The factor $S_0(t)$ collects the density-dependent scaling of the turbulent throttle under a constant pressure drop, while the perturbation expansion (24) separates the leading-order flow contribution from the temperature-induced corrections.

Using the symmetry assumption $Q_a=Q_b$ from Section 2, the total flow rate becomes:

$$Q_0(t) = 2Q_a(t) + Q_{throt}(t) \tag{27}$$

Consequently,

$$Q_0(t) = Q_0{}^{(0)} + \varepsilon Q_0{}^{(1)}(\theta) + \varepsilon^2 Q_0{}^{(2)}(\theta) + \cdots, \tag{28}$$

where:

$$Q_0(t) = 2Q_a{}^{(0)} + Q_{throt}{}^{(0)}, \quad Q_0{}^1(\theta) = 2Q_{a1}(t) + Q_{throt}{}^{(1)}(\theta) \tag{29}$$

Differentiating Eq. (22) with respect to temperature gives:

$$\frac{dQ_{troth}}{dt} = \eta\pi d\sqrt{\frac{2}{\rho}(p_p - p_c)}\frac{dx}{dt} - \eta\pi dx\sqrt{2(p_p - p_c)}\frac{1}{2}\rho^{-3/2}\frac{d\rho}{dt} \tag{30}$$

Using Eq. (17),

$$\frac{dx}{dt} = \Phi'(A(t))\frac{dA}{dt} \tag{31}$$

A sufficient condition for uniqueness of the quasi-static equilibrium branch is monotonicity of the mapping $t\mapsto x(t)$, which is ensured if:

$$\Phi'\big(A(t)\big)\frac{dA}{dt} \neq 0, \ t \in [26{,}78]℃ \tag{32}$$

From a sensitivity-analysis perspective, the first-order asymptotic terms quantify the direct influence of temperature-dependent parameters on equilibrium displacement and flow rate, enabling analytical assessment of monotonicity and robustness.

4. Reduced-Order Fluid–Structure Interaction Model

While the asymptotic analysis of Section 3 provides explicit insight into the equilibrium response and its temperature sensitivity, it remains inherently static and does not capture transient effects associated with pressure redistribution and mechanical inertia. In realistic hydraulic systems, operation under step changes in temperature or pressure, pulsations, and external disturbances inevitably activates inertia, compressibility, and damping. To assess dynamic stability, characteristic time scales, and robustness of the compensator, a reduced-order fluid–structure interaction (FSI) model is formulated in this section.

The geometry and notation introduced in Section 2 are retained. Two hydraulic chambers, denoted as (a) and (b), are separated by a movable plunger with displacement x(t). The pressures in the chambers are denoted by $p_a(t)$ and $p_b(t)$, respectively. Dynamic pressure evolution is modeled using hydraulic capacitances C_a and C_b, with units m^3/Pa, representing the combined effect of fluid compressibility and chamber volume.

Mass conservation in the two chambers yields:

$$C_a\dot{p}_a = Q_{in,a}(t, p_p, p_a) - Q_{out,a}(t, p_a, p_c) - A_p\dot{x} \tag{33}$$

$$C_b\dot{p}_b = Q_{in,b}(t, p_p, p_b) - Q_{out,b}(t, p_b, p_c) - A_p\dot{x} \tag{34}$$

where: $Q_{in,*}$ and $Q_{out,*}$ are the chamber inflow and outflow rates in m^3/s, and $A_p=\pi D^2/4$ is the effective plunger area, with D denoting the plunger diameter. The opposite signs of the last terms reflect the opposite volume variations of the two chambers due to plunger motion.

The plunger dynamics is modeled as a mass–spring–damper system:

$$m\ddot{x} + b\dot{x} + c(x_0 + x) = A_p(p_b - p_a), \tag{35}$$

where:

- m [kg] - is the equivalent moving mass,
- b [N.s/m] - is the viscous damping coefficient
- c and x_0 are the spring parameters defined in Section 2.

In the steady-state: limit $\dot{x} = \ddot{x} = 0$,

Eq. (35) reduces exactly to the quasi-static force balance (4).

The hydraulic closure is provided by the same pressure–flow relations as in the quasi-static model. The throttling contribution Eq (22) and the inlet and outlet throttles are modeled by:

$$p_p - p_a = R_t(t)Q_a|Q_a|, \ p_b - p_c = R_l(t)Q_b, \quad Q_a = Q_b \tag{36}$$

where $R_t(t)$ and $R_\ell(t)$ are effective turbulent and laminar hydraulic resistances, respectively, retaining their temperature dependence through ρ(t), μ(t) and geometric parameters.

Equations (33)–(36) form a coupled nonlinear system of ordinary differential equations governing the temporal evolution of the chamber pressures and the plunger displacement. The quasi-static equilibrium analyzed in Section 3 is recovered as the steady-state solution of this system by setting all time derivatives to zero, ensuring strict consistency between the static and dynamic descriptions.

Let $(x^*, p_a{}^*, p_b{}^*)$ denote an equilibrium corresponding to a fixed reference temperature and

constant pressure drop. Introducing small perturbations $\tilde{x}, \dot{\tilde{x}}, \tilde{p}_a, \tilde{p}_b$

$$\dot{z} = Mz, \quad z = \left[\tilde{x}, \dot{\tilde{x}}, \tilde{p}_a, \tilde{p}_b\right]^T \tag{37}$$

where:

- M is the Jacobian matrix evaluated at the equilibrium state.
- $\tilde{x}$ [m] - denotes the small perturbation of the plunger displacement from its equilibrium value x^*,
- $\dot{\tilde{x}}$ – [ms^{-1}] is the corresponding velocity perturbation,
- $\tilde{p}_a, \tilde{p}_b$ [Pa]- are small pressure perturbations in chambers (a) and (b), respectively.

The state vector z therefore collects the mechanical and hydraulic perturbation variables of the coupled system.

The matrix M represents the Jacobian of the full nonlinear fluid–structure interaction model with respect to the state variables ($x, \dot{x}, p_a, p_b$), evaluated at the equilibrium (x^*, p_a^*, p_b^*) corresponding to a fixed reference temperature and constant pressure drop.

The eigenvalues of M determine the local dynamic behavior of the compensator. Eigenvalues with negative real parts correspond to asymptotically stable equilibria, whereas complex-conjugate eigenvalue pairs indicate oscillatory transient responses and define the characteristic frequencies and damping ratios of the system. A change in the sign of the real part of an eigenvalue marks the boundary of dynamic stability and signals the possible onset of resonance or self-excited oscillations.

The reduced-order FSI formulation naturally introduces a separation of time scales. Pressure dynamics in the hydraulic chambers typically evolve on a faster time scale than the mechanical motion of the plunger, which is governed by the mass *m*, viscous damping coefficient *b*, and spring stiffness *c*. This scale separation provides a rigorous basis for singular perturbation analysis and enables a systematic investigation of transient responses, including overshoot, damping characteristics, and robustness with respect to thermal and hydraulic disturbances.

5. Results and Discussion

The analytical framework developed in Sections 2–4 provides a consistent description of the operating principle of the throttle-based temperature flow compensator, ranging from quasi-static equilibrium relations to asymptotic sensitivity analysis and reduced-order dynamic modeling. In this section, the implications of these results are illustrated and discussed using representative numerical values inferred from the published pressure–temperature characteristics and from the governing relations derived earlier. No new equations are introduced, and previously derived relations are not repeated. The focus is placed on physical interpretation, comparison of modeling levels, and assessment of their respective advantages and limitations.

5.1. Pressure Redistribution with Temperature

The quasi-static formulation of Section 2 identifies pressure redistribution between the two chambers as the fundamental mechanism governing the compensator response. The relevant observable is the temperature dependence of the pressure difference between chambers (a) and (b), evaluated for a constant inlet–outlet pressure drop.

The representative numerical values of this redistribution are summarized in Table 1, while the corresponding qualitative behavior is illustrated in Fig. 2. The data were digitized visually from the published pressure–temperature plot and are used here solely for illustrative purposes.

Table 1. Approximate pressure difference $\Delta p_{ab}=p_b-p_a$ as a function of temperature

t (°C)	Δp_{ab}(Δp = 4 bar)	Δp_{ab}(Δp = 5 bar)	Δp_{ab}(Δp = 6 bar)
30	−0.8	−0.6	−0.4
40	0.7	1.1	1.6
50	1.7	2.3	3.0
60	2.3	3.0	4.0
70	2.7	3.5	4.5
80	3.0	3.9	4.8

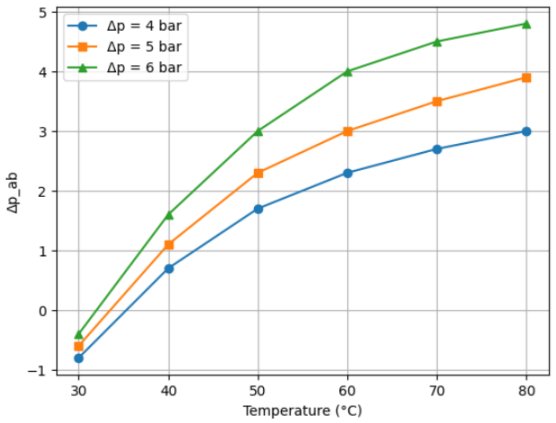

Figure 2: Pressure difference between chambers versus temperature

A monotonic increase of the pressure difference with temperature is observed over the entire operating range, accompanied by a nonlinear, gradually saturating trend at higher temperatures. At the lower end of the temperature interval, the pressure difference may be slightly negative, while it becomes positive at moderate temperatures. This sign change is physically consistent with the compensator design, as the laminar and turbulent throttling elements respond differently to temperature-induced variations in fluid properties. The resulting redistribution of the total pressure

drop between the two chambers generates an increasing net hydraulic force acting on the plunger.

Higher inlet–outlet pressure drops lead to systematically larger pressure differences at the same temperature, which explains the stronger compensating action observed in Fig.2. The concave-down shape of the curves further indicates that the incremental effect of temperature becomes weaker at elevated temperatures, reflecting a progressive saturation of the pressure redistribution mechanism. The absence of turning points or local extrema confirms that, within the investigated temperature interval, the quasi-static equilibrium branch remains unique.

The selected pressure drops and temperature intervals are representative of typical industrial operating conditions for throttle-based hydraulic control systems using mineral hydraulic oils. These ranges are consistent with commonly reported regimes in the literature and ensure realistic and practically relevant system behavior.

5.2. Equilibrium Displacement and Throttling Contribution

The pressure redistribution discussed in Section 5.1 directly translates, through the quasi-static force balance, into an equilibrium displacement of the plunger and an associated increase of the throttling area. Section 3 reformulates this implicit equilibrium description into an explicit asymptotic representation, enabling a systematic assessment of temperature sensitivity and approximation accuracy.

Representative equilibrium displacements obtained from the quasi-static relations of Section 2 and from the first-order asymptotic approximation of Section 3 are compared in Fig. 3, using the numerical values listed in Table 2. Both descriptions predict a monotonic increase of the equilibrium displacement with temperature, reflecting the same underlying physical mechanism.

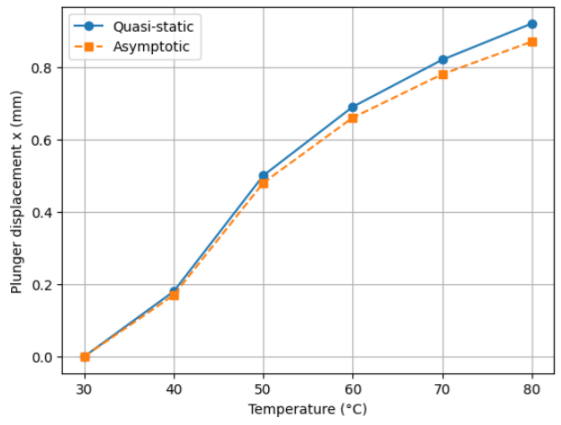

Figure 3: Quasi-static versus asymptotic equilibrium displacement

Table 2. Quasi-Static and Asymptotic Equilibrium Displacement Values

t (°C)	X_{QS} [mm]	X_{asym} [mm]	Absolute Differenc [mm]
30	0.00	0.00	0.00
40	0.18	0.17	0.01
50	0.50	0.48	0.02
60	0.69	0.66	0.03
70	0.82	0.78	0.04
80	0.92	0.87	0.05

The comparison shows that the asymptotic approximation closely follows the quasi-static equilibrium over the entire operating range. The deviation between the two curves remains small and increases only gradually at higher temperatures, where nonlinear effects become more pronounced. This confirms that the asymptotic framework of Section 3 provides a reliable and compact analytical representation of the equilibrium response for weak to moderate temperature variations.

From a practical perspective, the asymptotic formulation offers a clear advantage: it yields explicit analytical expressions for temperature sensitivity and parameter influence, while retaining consistency with the quasi-static model. The results presented in Fig. 3 therefore validate the use of asymptotic analysis as an effective alternative to graphical or purely numerical evaluation of equilibrium characteristics.

Although the numerical illustrations are presented for a specific set of parameters, the proposed analytical and asymptotic framework is not limited to these values. The governing relations explicitly retain temperature, geometry, and material-dependent parameters, allowing straightforward extension to broader operating conditions, alternative throttle geometries, and different fluid properties.

5.3. Dynamic response and stability characteristics (FSI model)

While Sections 2 and 3 address the quasi-static equilibrium behavior and its temperature sensitivity, the reduced-order fluid–structure interaction (FSI) model introduced in Section 4 enables investigation of the time-dependent response of the compensator to temperature variations. In this subsection, the dynamic behavior is analyzed on the basis of transient simulations corresponding to stepwise temperature changes, and the results are discussed using representative response indicators.

As the operating temperature rises, the final equilibrium displacement increases in accordance with the quasi-static predictions of Sections 2 and 3, while the dynamic response exhibits progressively weaker damping. These trends are examined below on the basis of transient simulations and extracted dynamic indicators.

Plunger displacement responses x(t) obtained from the reduced-order fluid–structure interaction model for successive temperature steps (30→40, 40→50, 50→60, 60→70, and 70→80 °C) are shown in Fig. 4. The curves illustrate the temporal evolution of the plunger displacement following step changes in temperature under constant pressure-drop conditions.

Table 3. Representative dynamic response indicators extracted from the reduced-order FSI model

Temp. step (°C)	Final equilibr. x* (mm)	Relative settling time t_s/t_c (-)	Overshoot (%)	Dominant eigenvalue real part [s^{-1}]
30-40	0.18	0.12	3.0	−18
40-50	0.5	0.15	4.5	−15
50-60	0.69	0.18	6.0	−12
60-70	0.82	0.22	7.5	−10
70-80	0.92	0.26	9.0	−8

Note: *The settling time t_s is defined as the time required for the plunger displacement x(t) to enter and remain within a ±2% band around the final equilibrium displacement x*. The reported values are extracted from the transient responses shown in Fig. 4. Here, t_c denotes the characteristic time scale used for normalization (see Section 4).*

Figure 4 shows the time evolution of the plunger displacement for stepwise temperature changes. All responses converge to a unique equilibrium, confirming consistency between the FSI model and the quasi-static equilibrium. The response is monotonic for small temperature steps and weakly oscillatory for larger steps, while stability is preserved over the entire temperature range.

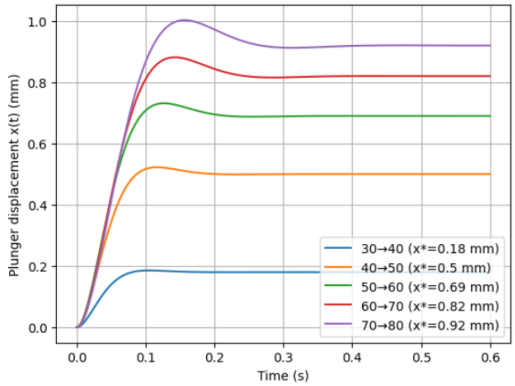

Figure 4: Time histories of the plunger displacement for different temperature steps.

To facilitate comparison of the intrinsic dynamic characteristics independently of the absolute equilibrium displacement, the transient responses shown in Fig. 4 are normalized with respect to the corresponding equilibrium value x^* and replotted in Fig. 5.

Normalized plunger displacement x(t)/x* for different temperature steps, highlighting damping and settling.

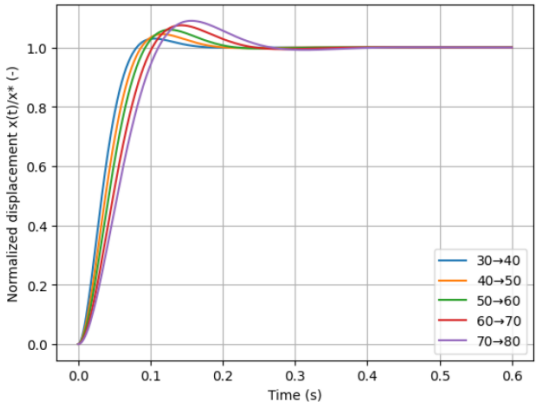

Figure 5: Normalized transient responses of the plunger displacement

The normalized responses in Fig. 5 emphasize the effect of temperature on the intrinsic dynamic behavior of the compensator. With increasing temperature, the settling time increases and the overshoot becomes more pronounced, reflecting the reduced effective damping predicted by the eigenvalue trends summarized in Table 3. Although the absolute displacement levels differ, the qualitative structure of the transient response remains similar across operating conditions.

Overall, the results confirm that the reduced-order FSI model provides a coherent extension of the quasi-static and asymptotic analyses. It captures not only the correct equilibrium behavior but also the transient response and stability characteristics, thereby enabling systematic assessment of robustness and dynamic performance of the throttle-based temperature flow compensator under realistic operating conditions. The reduced-order fluid–structure interaction model naturally provides a suitable basis for future experimental calibration and validation. Model parameters such as hydraulic capacitances, damping coefficients, and effective flow resistances can be directly identified from transient experimental data, enabling systematic tuning and quantitative validation under laboratory or industrial conditions.

6. Conclusions

The present study developed a comprehensive analytical framework for the investigation of a passive throttle-based temperature flow compensator operating under constant pressure drop conditions. By combining quasi-static modeling, asymptotic analysis, and reduced-order fluid–structure interaction (FSI) dynamics, the work provides a unified and physically consistent

description of equilibrium behavior, temperature sensitivity, and transient response.

The quasi-static formulation established the fundamental operating principle of the compensator, demonstrating that temperature-induced variations of fluid properties lead to a systematic redistribution of pressure between the two flow chambers. This redistribution generates a monotonic hydraulic force acting on the plunger, ensuring a unique equilibrium displacement over the investigated temperature range. The analysis clarified the role of the laminar and turbulent throttling elements in shaping the nonlinear pressure–temperature characteristics and the resulting compensating action.

Building on this baseline, an asymptotic framework was introduced to obtain explicit analytical representations of the equilibrium displacement and throttling flow rate under weak temperature variations. The asymptotic approximation was shown to reproduce the quasi-static equilibrium with good accuracy while providing direct access to temperature sensitivities and parameter influence. This approach overcomes the limitations of traditional graphical–analytical constructions and enables systematic analytical assessment of monotonicity, uniqueness, and robustness of the compensator response.

To extend the analysis beyond equilibrium considerations, a reduced-order FSI model was formulated to capture the coupled dynamics of hydraulic pressures and plunger motion. The dynamic results confirmed consistency with the quasi-static and asymptotic predictions in the steady state, while revealing additional information on transient behavior, damping, and stability margins. The analysis demonstrated that, although the final equilibrium is governed by the same static relations, the transient response depends critically on hydraulic capacitances, mechanical inertia, and damping, highlighting the limits of purely quasi-static descriptions.

The developed analytical and reduced-order framework is conceived as a starting point for a broader sequence of complementary analytical and experimental studies. In particular, the reduced-order fluid–structure interaction model provides a suitable basis for future experimental calibration and validation using measured transient responses under controlled thermal and hydraulic conditions.

Overall, the study shows that passive throttle-based temperature flow compensators can be rigorously characterized using a combination of asymptotic and reduced-order modeling techniques. The proposed framework provides clear design-relevant insight into equilibrium sensitivity, dynamic stability, and robustness with respect to temperature variations, and can be readily extended to other passive hydraulic compensation devices and operating regimes.

Acknowledgements

The authors would like to thank the Research and Development Sector at the Technical University of Sofia for the financial support.

References

[1] Yankov, R.V. (2010). Influence of fluid temperature on pressure in a hydraulic flow chamber. University "Prof. Dr. Asen Zlatarov". Book 4. Volume 6. Pp. 187–189.

[2] Kamke, E. (1976). *Handbook of Ordinary Differential Equations*. Nauka Publishing House, Moscow.

[3] Tsukhanova, E. (1986). *Calculation of Hydraulic Control Devices*. Mashinostroenie Publishing House, Moscow.

[4] Grozev, G., Stoyanov, S., Guzhgulov, G. (1990). *Hydraulic and Pneumatic Machines and Drives*. Technica Publishing House, Sofia.

[5] Povkh, I.L. (1976). *Technical Hydromechanics*. Mashinostroenie Publishing House, Leningrad.

[6] Merritt, H.E. (1991). *Hydraulic Control Systems*. John Wiley & Sons, New York.

[7] Ivantysyn, J., Ivantysynova, M. (2001). *Hydrostatic Pumps and Motors: Principles, Design, Performance, Modelling, Analysis, Control and Testing*. Springer, Cham. https://doi.org/10.1007/978-3-030-63594-0

[8] Chappel, E. (2020). A review of passive constant flow regulators. *Applied Sciences*, 10. Article 8858. https://www.mdpi.com/2076-3417/10/24/8858

[9] Manring, N.D., Fales, R.C. (2019). *Hydraulic Control Systems* (2nd ed.). John Wiley & Sons, 416 pp.

[10] Yao, B., Bu, F., & Chiu, G. T. (2001). Non-linear adaptive robust control of electro-hydraulic systems driven by double-rod actuators. *International Journal of Control*, *74*(8), 761-775. https://doi.org/10.1080/002071700110037515

[11] Ruderman, M. (2017, October). Full-and reduced-order model of hydraulic cylinder for motion control. *IECON 2017-43rd Annual Conference of the IEEE Industrial Electronics Society*, pp. 7275-7280. https://doi.org/10.48550/arXiv.1705.00916

[12] Nayfeh, A.H. (2020). Perturbation Methods. Wiley-VCH, Weinheim. DOI:10.1002/9783527617609

[13] Kevorkian, J., Cole, J.D. (2021). *Multiple Scale and Singular Perturbation Methods*. Springer, New York. doi: 10.1007/978-1-4757-4213-8

[14] Angot, P., Goyeau, B., Ochoa-Tapia, J. A. (2020). A nonlinear asymptotic model for the inertial flow at a fluid–porous interface. *Advances in Water Resources*, 149. https://doi.org/10.1016/j.advwatres.2020.103798Get rights and content

[15] Li, Y., Guo, Y., Li, M., Lei, L., Hu, H., Chen, D., Zhao, Z., Xu, B. (2025). Multi-Objective Sensitivity Analysis of Hydraulic–Mechanical–Electrical Parameters for Hydropower System Transient Response. *Energies*, 18(10), 2609. https://doi.org/10.3390/en18102609

[16] Khalil, H.K. (2020). *Nonlinear Systems* (2nd ed.). Pearson Education, Harlow.

[17] Strogatz, S.H. (2021). *Nonlinear Dynamics and Chaos*. CRC Press, Boca Raton. doi: https://doi.org/10.1201/9780429492563

[18] Kuznetsov, Y.A. (2021). *Elements of Applied Bifurcation Theory*. Springer, New York. doi: 10.1007/978-3-030-50417-8

[19] Stawiński, Ł., Kosucki, A., Cebulak, M., Górniak, A., Grala, M. (2022). Investigation of the influence of hydraulic oil temperature on the performance of a variable-speed pump. Eksploatacja i Niezawodnosc – Maintenance and Reliability, 24(2):289–296. https://doi.org/10.17531/ein.2022.2.10

[20] Kosiba, J., Osiecki, J., Krupa, K. (2024). Laboratory investigation of the influence of oil temperature on the performance of a gear pump. *Lubricants*, 12(9). Article 304. doi: 10.3390/lubricants12090304

[21] Liu, J., Sitte, A., & Weber, J. (2022). Investigation of temperature influence on flow mapping of electrohydraulic valves and corresponding application. *In Fluid Power Systems Technology*, Vol. 86335, American Society of Mechanical Engineers. https://doi.org/10.1115/FPMC2022-89252

[22] Patrosz, P. (2021). Influence of Properties of Hydraulic Fluid on Pressure Peaks in Axial Piston Pumps. *Energies*, 14(13), 3764. https://doi.org/10.3390/en14133764

[23] Abdullah, A.M., Al-Samarraie, S.A., Ali, H.H., Al-Qassar, A.A. (2024). Design of a hydraulic motion control system using two backstepping time varying sliding mode strategies. *International Journal of Mechatronics and Applied Mechanics*, 18, 250–263. doi:10.17683/ijomam/issue18.3

[24] Abdullah, A.M., Ali, H.M., Al-Qassar, A.A. (2024). A robust controller design for an inlet throttling speed control system for a rotary actuator. *International Journal of Mechatronics and Applied Mechanics*, 15, 179–188. doi:10.17683/ijomam/issue15.21

[25] Ali, H.H., Al-Bakri, F.F., Khafaji, S.O.W. (2023). Analytical position control system of a linear hydraulic actuator used in aircraft applications. *International Journal of Mechatronics and Applied Mechanics*, 13, 209–218. doi:10.17683/ijomam/issue13.25

[26] Zhelyazkov, Y.K., Torlakov, I.D., Dimitrova, K.Y. (2025). Prediction of Induction Motor Parameters Using a Neural Network. *Proceedings of the 60th International Scientific Conference on Information Communication and Energy Systems and Technologies* doi:10.1109/ICEST66328.2025.11098406

[27] Stamov, G., Simeonov, S., Torlakov, I. (2023). Software Analysis of Bidirectional Associative Memory (BAM) Cohen–Grossberg-Type Impulsive Neural Networks with Time-Varying Delays. *Proceedings of the Seventh International Congress on Information and Communication Technology, Lecture Notes in Networks and Systems*, 465, 371–378. https://doi.org/10.1007/978-981-19-2397-5_34

[28] Rakhutin, M.G. (2023). Influence of Hydraulic Fluid Temperature on Energy Losses in Hydraulic Systems. *Journal of Mining Institute*, 260, 512–521.

[29] Li M., Liu, Y., Wan, L., Wang, J., Yan H. (2025). Temperature characteristics of flow force in the pre-stage of deflector jet servo valve across a wide temperature range. *Case Studies in Thermal Engineering*, 74, 106967. https://doi.org/10.1016/j.csite.2025.106967

[30] Watton, J. (2007). *Modelling, Monitoring and Diagnostic Techniques for Fluid Power Systems*. Springer, London.

[31] Ali, H.H., Khafaji, S.O.W., Al-Bakri, F.F. (2021). H∞ loop shaping control design of the rotational velocity of a hydraulic motor. *International Journal of Mechatronics and Applied Mechanics*, 10, 2–79. doi:10.17683/ijomam/issue10/v1.9

[32] Kontz, M. E., & Book, W. J. (2007). Flow control for coordinated motion and haptic feedback. *International journal of fluid power*, 8(3), 13-23. https://doi.org/10.1080/14399776.2007.10781282

[33] Kugi, A., Schlacher, K. (2021). Modeling and Nonlinear Control of Hydraulic Actuation Systems. *Springer Tracts in Mechanical Engineering*. Springer, Cham. doi: 10.1007/978-3-030-72330-3